Comparative models of the EM-37 system with
MultiLoop III, VHPlate and Maxwell.

June 2006

In these examples, the response of MultiLoop III is compared with two other electromagnetic simulation algorithms, VHPlate (a component of Emigma), and Maxwell. This study compares the results from the three modeling algorithms. The contributions made by Richard Smith (VHPlate modeling) and Bob Lo (Maxwell modeling) are gratefully acknowledged.

All three are numerical simulation packages that run on personal computers, and each uses a different scattering algorithm. Maxwell uses concentric thin filaments to represent current flow in a perfectly resistive medium. This is the same technique as is used in MultiLoop II. In VHPlate, polynomial basis functions are used to represent the secondary excitation on the conductor, while in MultiLoop III, excitation is represented by local basis functions representing the stream potential of the surface current density at each location.

Each modeling algorithm is limited by the representation of the current excitation used in the numerical model. In MultiLoop III and Maxwell, the currents are limited by the assumption that the excitation occurs in pure inductive vortices. The accuracy of Maxwell further depends on the ability of the modeler to correctly predict the location of the filaments used to represent the currents. In VHPlate, the accuracy of the solution depends on how well the polynomial basis functions used in the solution represent the incident and scattered fields. VHPlate can slightly underestimate the excitation because the polynomial basis functions “leave out” part of the incident field, particularly when the exciting field exhibits large variation over the conductor. However, the excitation in VHPlate is not limited to induction only, but included current channeling. As is illustrated Figure 8, channelling can enhance the anomalous response even in very resistive background media.

The cases illustrated were chosen so all algorithms would perform well. MultiLoop III has geometric and physical capabilities not present in the Maxwell and VHPlate. It would be pointless to conduct a study where the physical basis of the other algorithms did not apply.

The constraints on the geometrical representation of the currents in VHPlate and Maxwell are not present in MultiLoop III. In the examples that follow, the MultiLoop III response has been computed with 131 basis functions. However, models with over 2000 basis functions have been computed. Higher numbers of basis functions are preferable when the receiver is close to the conductor.

In the examples that follow, note that MultiLoop generates dB/dt, while VHPlate generated the coil response, –dB/dt, resulting is a reversal of the profiles. The model parameters employed are listed in the appendix.

Examples:

In Figures 1, 2 and 3 the response of MultiLoop III is compared with VHPlate for a plate with a top 100 meters, 200 meters and 50 meters deep. In this example, current channeling has been suppressed VHPlate by using a background medium with a resistivity of 10^6 ohm-m.

It is notable that the computation time required by VHPlate to calculate these model is approximately 6 minutes, while the same calculations took less than 30 seconds with MutliLoop III.

For the 100 meter plate (Figure 1) the peak response from MultiLoop III is approximately the same as VHPlate, 0.59 nT/sec..

In Figure 2, the plate has a top depth of 200 meters. Here the peak VHPlate response is approximately 0.043 nT/sec while MultiLoop III generates a response of 0.42 nT/sec. Again the match in the peak values is very good.

Figure 3 illustrates the response at 50 meters depth to top. VHPlate generates a peak response of approximately 3.4 nT/sec while MultiLoop III generates a response of 3.3 nT/sec. Given that the VHPlate data were read from the graphs illustrated in this report, the matches are excellent. In Figure 4, both produce peak responses of 19.1 nT/sec.

In Figure 5, Maxwell and MultiLoop III are compared for the plate at 100 meters depth. Maxwell generates a peak response of 0.583 nT/sec while MultiLoop III generates a response of 0.594 nT/sec. For the 10 meter plate Maxwell generates a peak response of 19.6 nT/sec, compared to MultiLoop III result of 19.1 nT/sec.

The excellent early time matched indicate that the inductive limit response is correct in all three modeling algorithms for the models studies. However, when the source is brought closer to the conductor, the quality of the inductive limit response should vary.

The decays are plotted in Figure 5 for the 100 meter deep plate and in Figure 6 for the 10 meter deep plate. The matches in Figure 5 are excellent; in Figure 6 Maxwell generates a decay that is faster than the decays generated by VHPlate and MultiLoop III. A possible explanation for the more rapid decay is that the bottoms of the current filaments used to represent the scattered currents in Maxwell are not in the locations the scattering currents in the conductor would be, but are on average too deep. This would cause an apparent more rapid decay at late time due to the geometric effect of the currents being on average too far from the receiver. The cause of the more rapid decay in Maxwell is likely to be a geometric effect because the decays computed for the 100 meter plate do not show this effect, but are virtually coincident with the values generated by MultiLoop III.

Finally, in Figure 8, the effect of anomaly enhancement, even in a resistive background is examined. Example IV is identical to Example I, except that a background of 10^3 ohm-m is used. In this example, the peak response generated by VHPlate is increased to approximately 0.68 nT/sec from approximately 0.58 nT/sec in the earliest time. Thus, current chanelling can enhance anomaly amplitudes even in very resistive background media, an effect to be noted when using MultiLoop III to model geophysical data.

***Figure 1:* MultiLoop III & VHPlate comparison, top of plates at 100 meters**
Mlp III

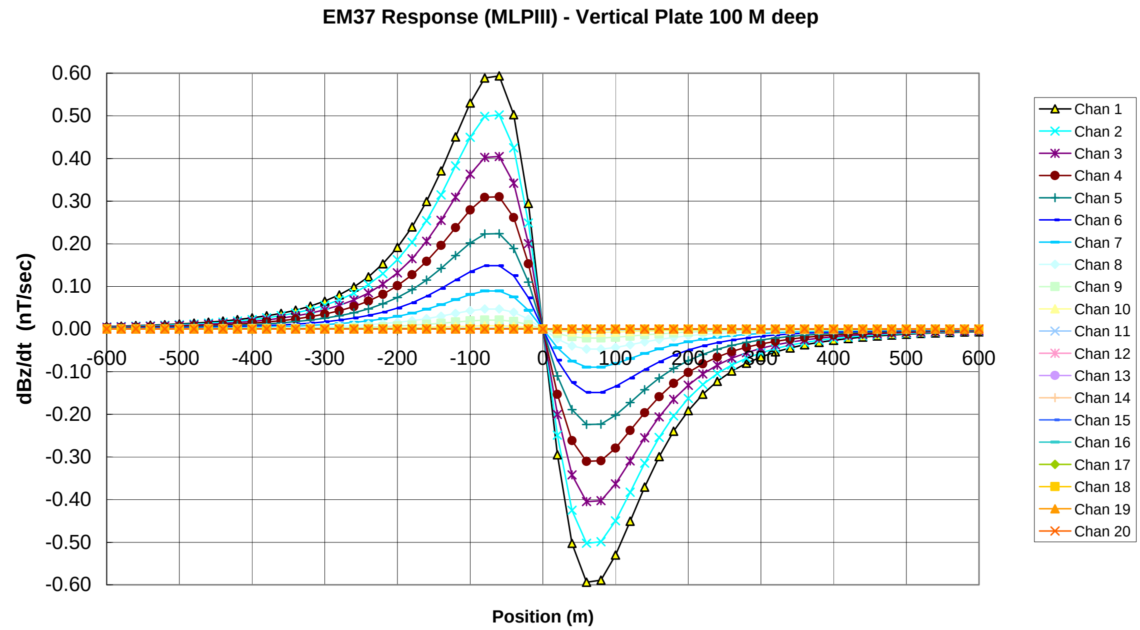

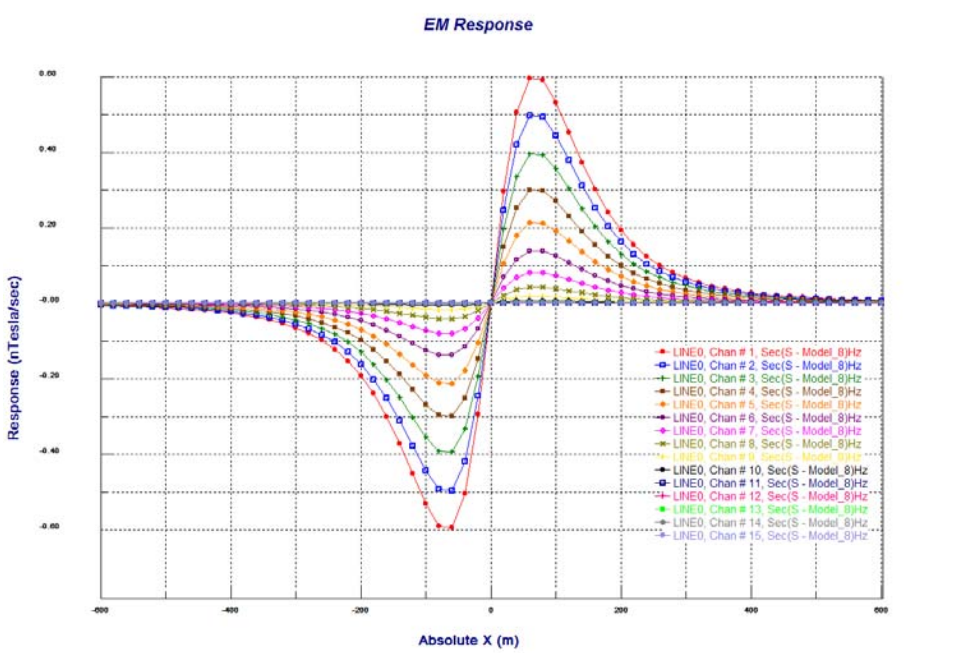

VH

Figure 2: **MultiLoop III & VHPlate comparison, top of plates at 200 meters**
MLP III

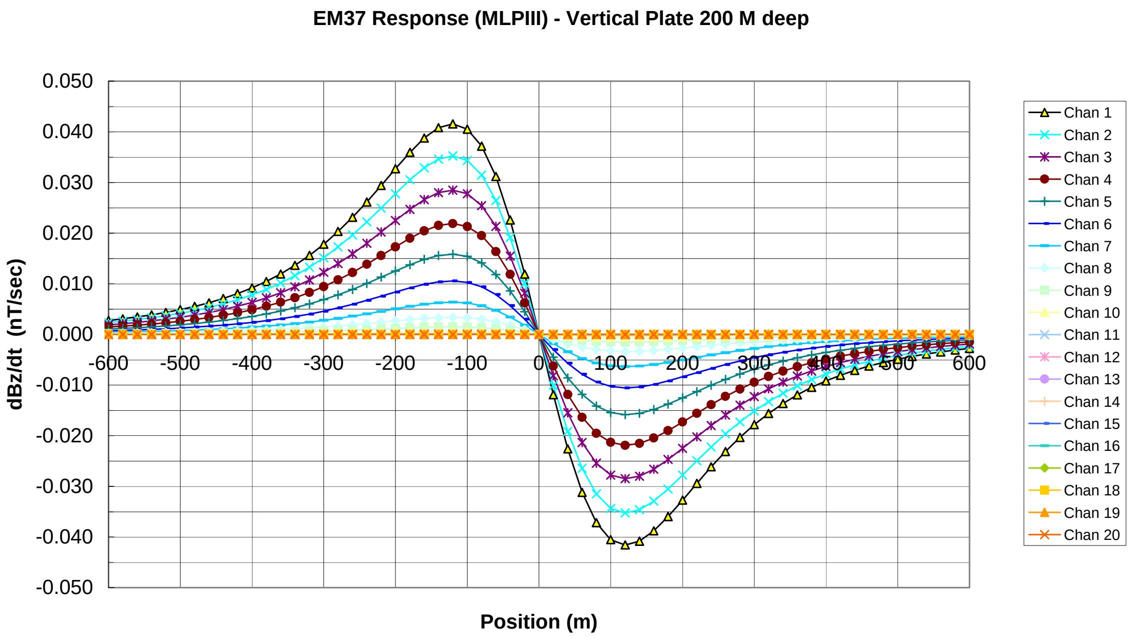

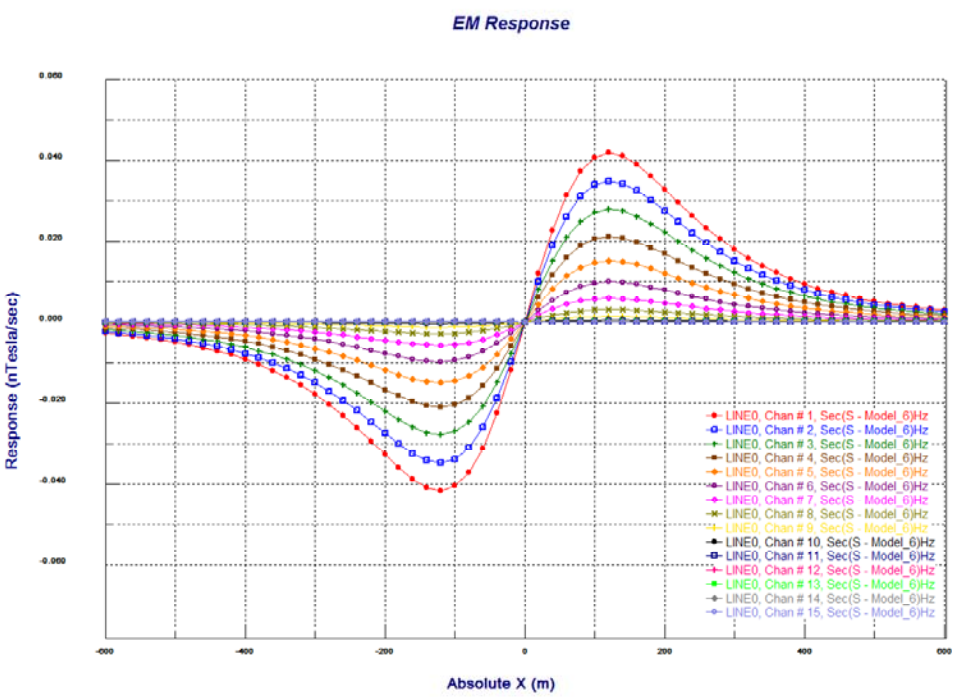

VH

Figure 3: **MultiLoop III & VHPlate comparison, top of plates at 50 meters**
MLP III

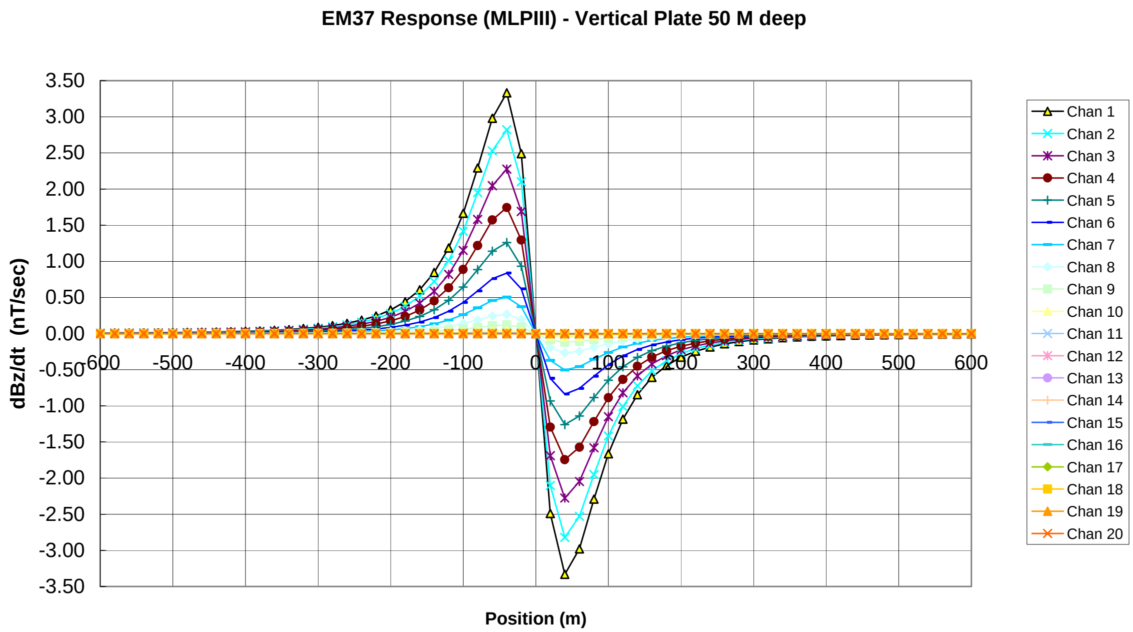

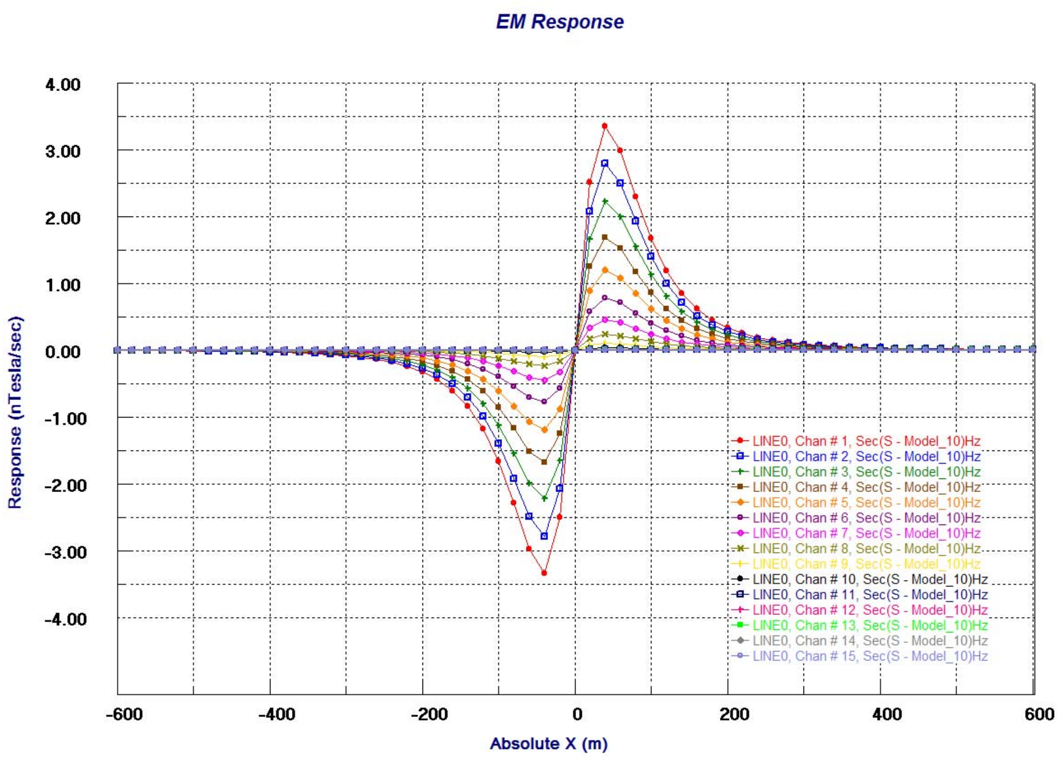

Figure 4: **MultiLoop III & VHPlate comparison, top of plates at 10 meters**

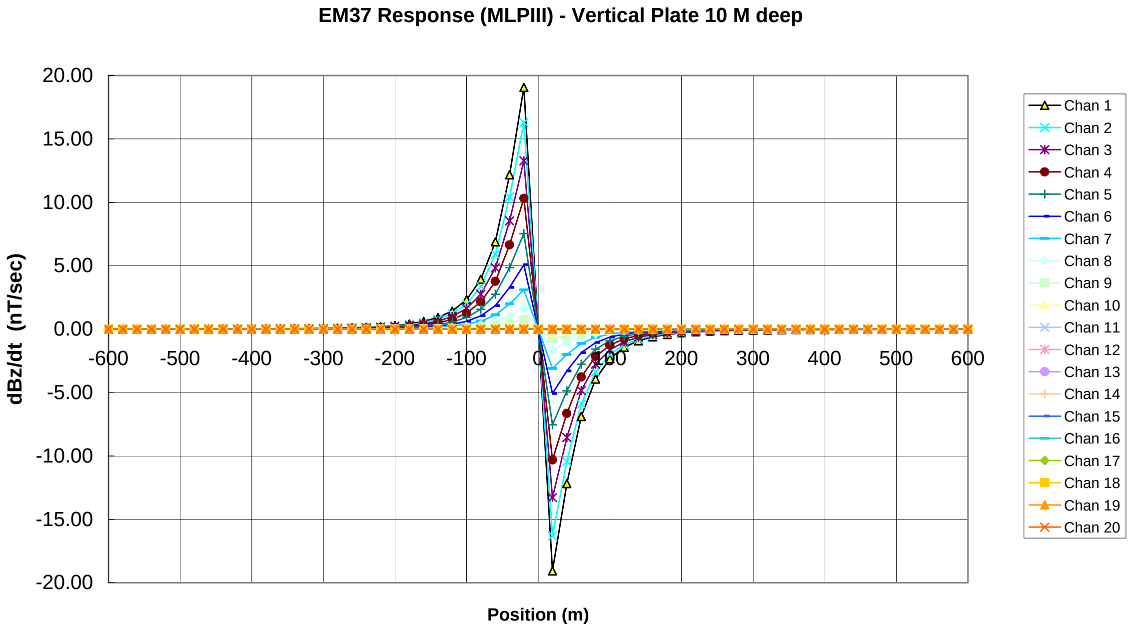

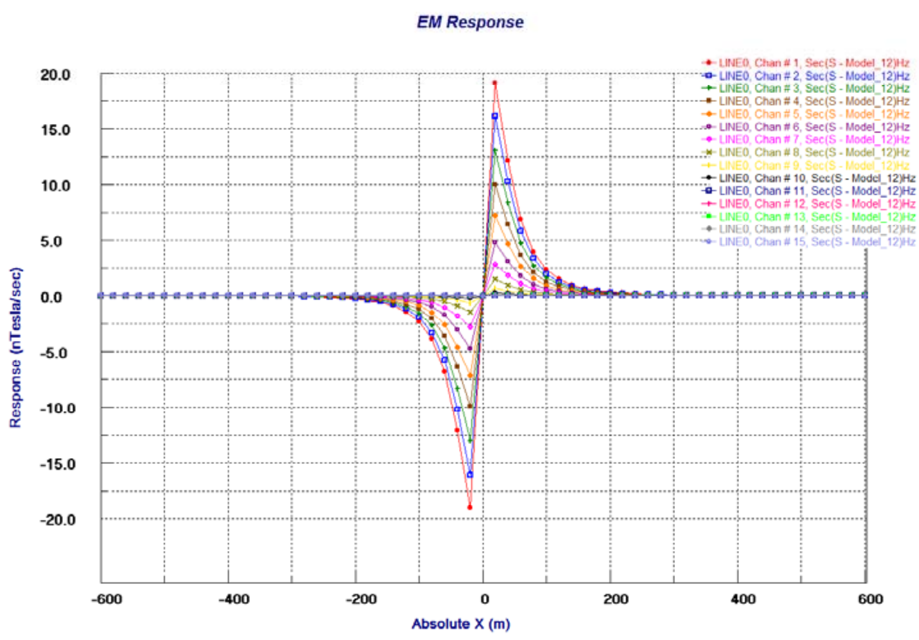

Figure 5: Comparison of MultiLoop III and Maxwell, 100 m & 10 m deep plates

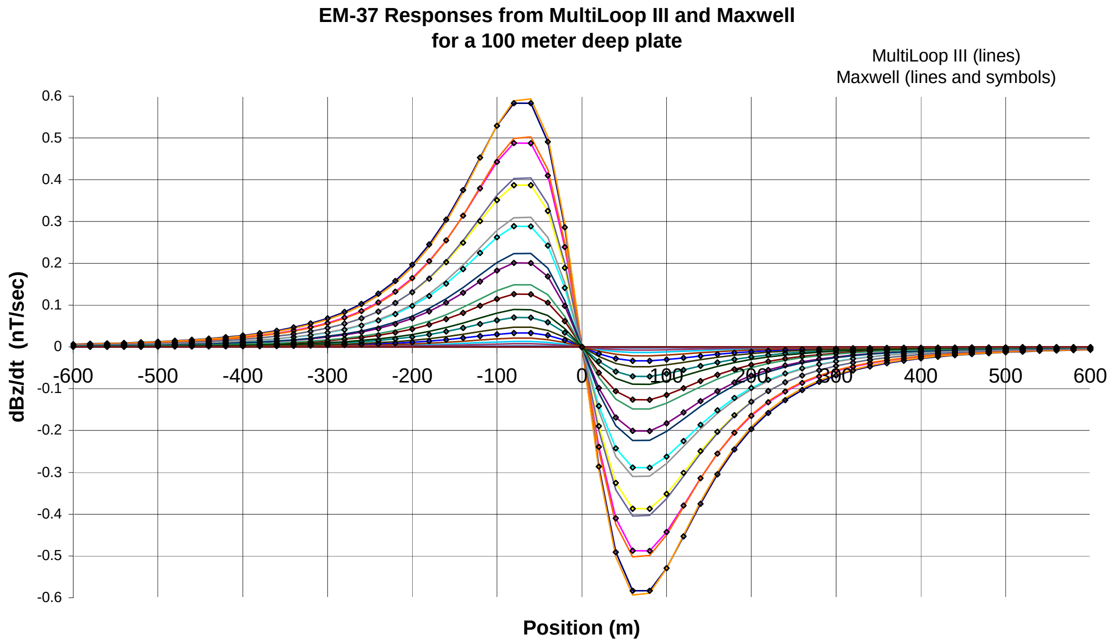

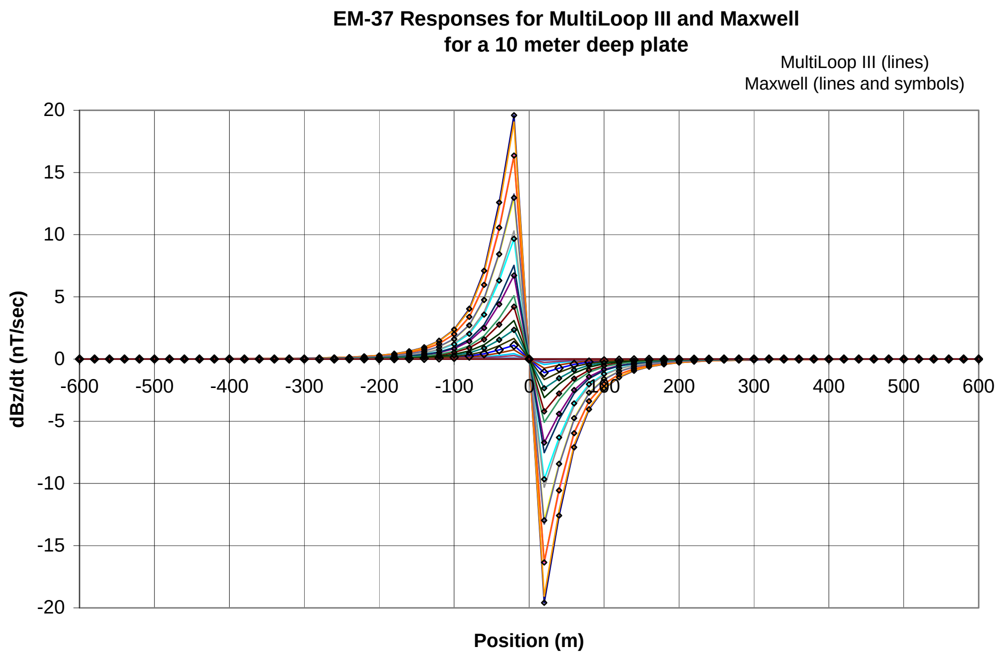

***Figure 6*: Comparison of decays from MultiLoop III, VHPlate and Maxwell at station 60, 100 m deep plate**

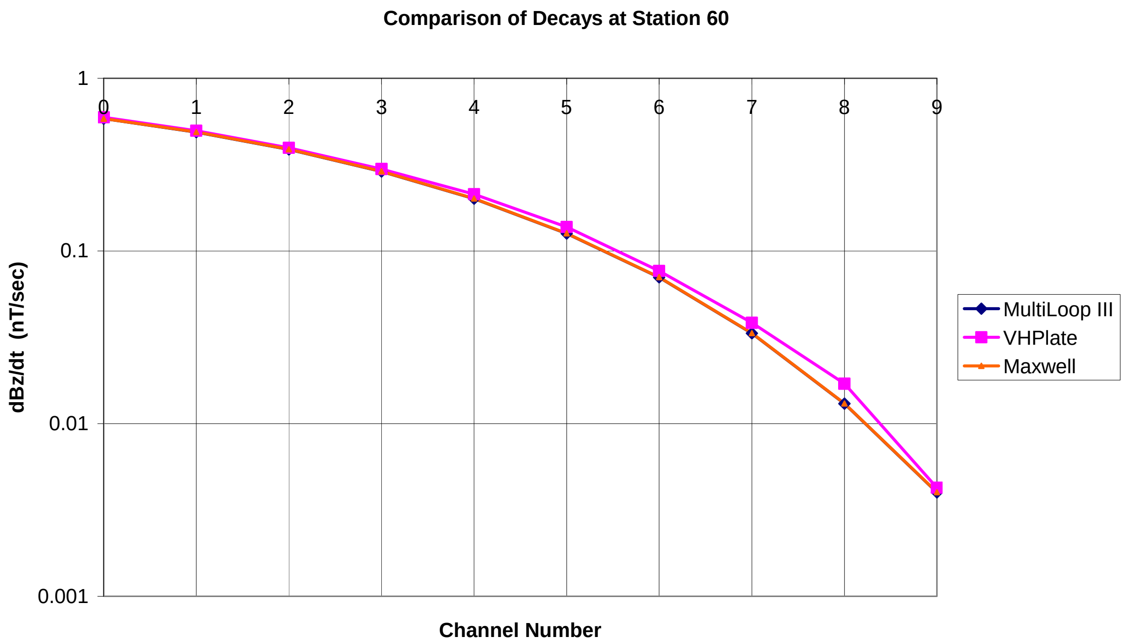

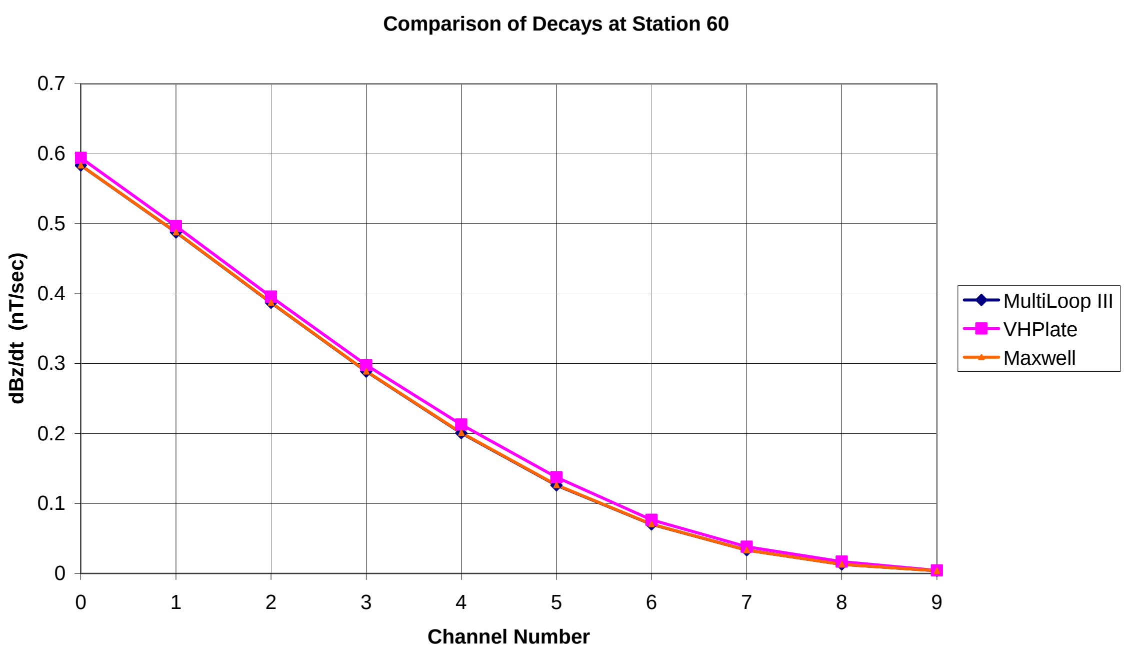

Figure 7: **Comparison of decays from MultiLoop III, VHPlate and Maxwell at station 20, 10 m deep plate**

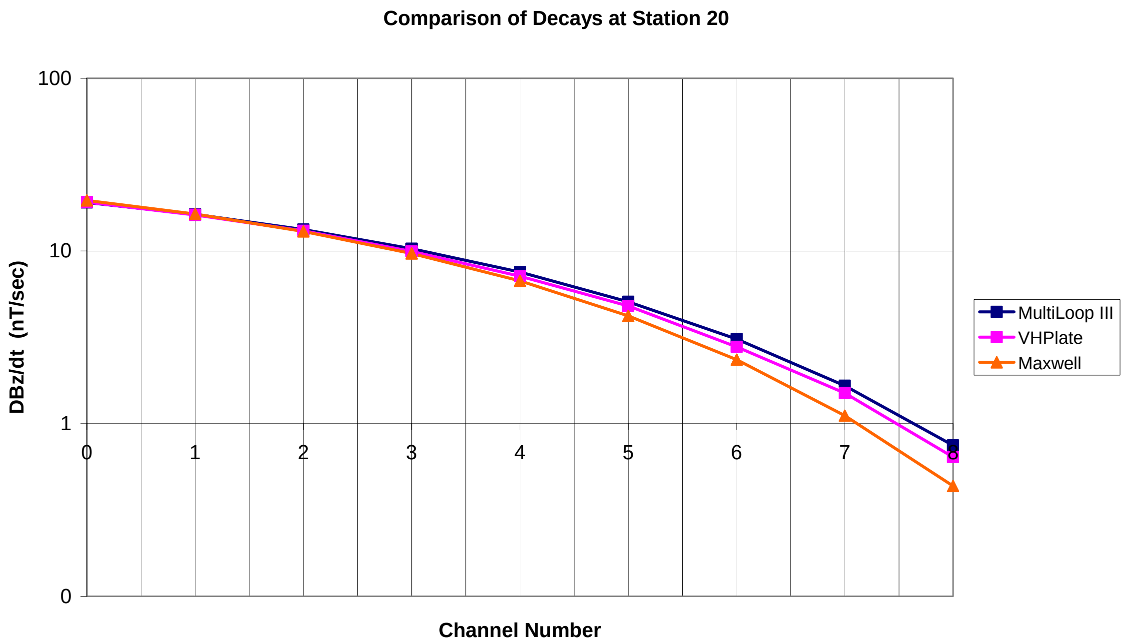

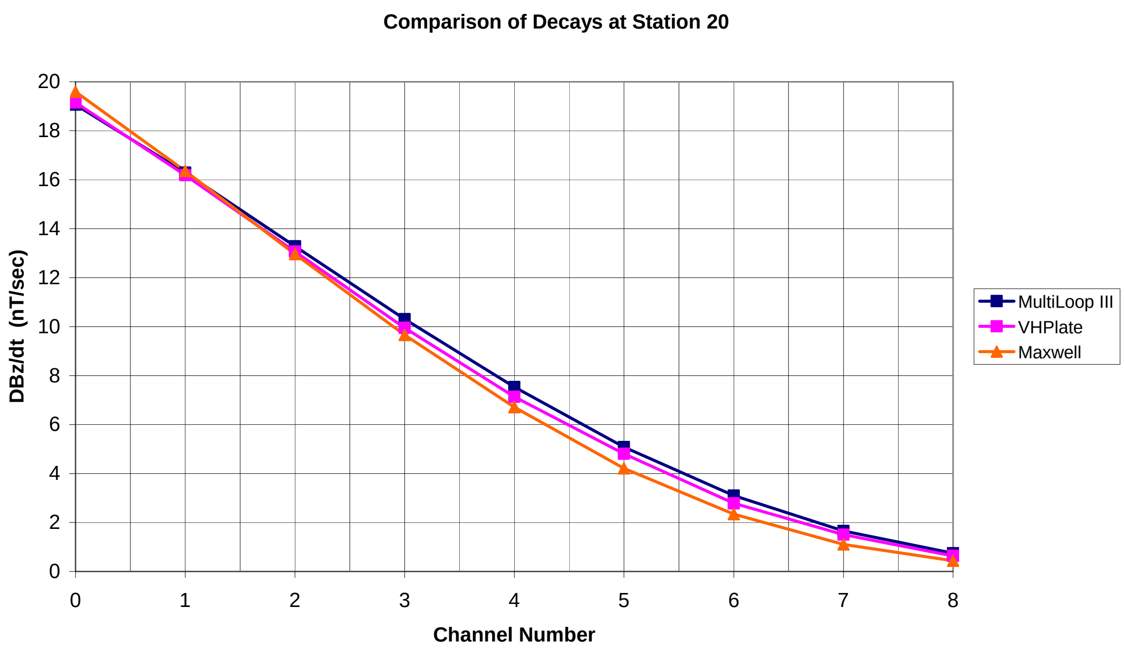

Figure 8: **Conductive Background - VH & MultiLoop III, top of plates at 100 meters**
Mlp III

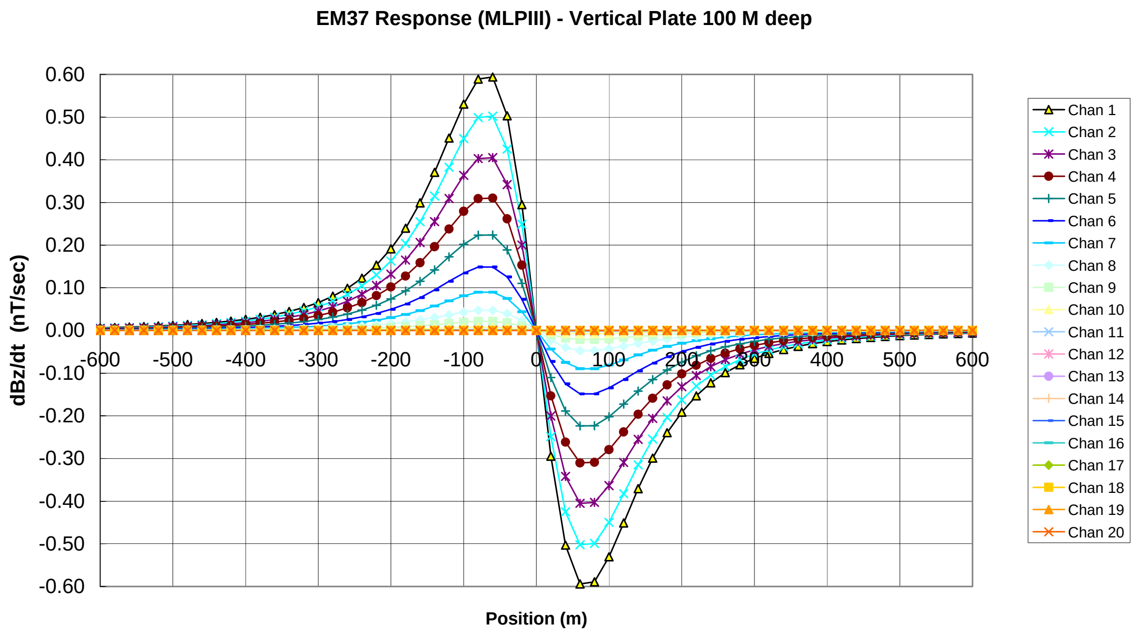

VH

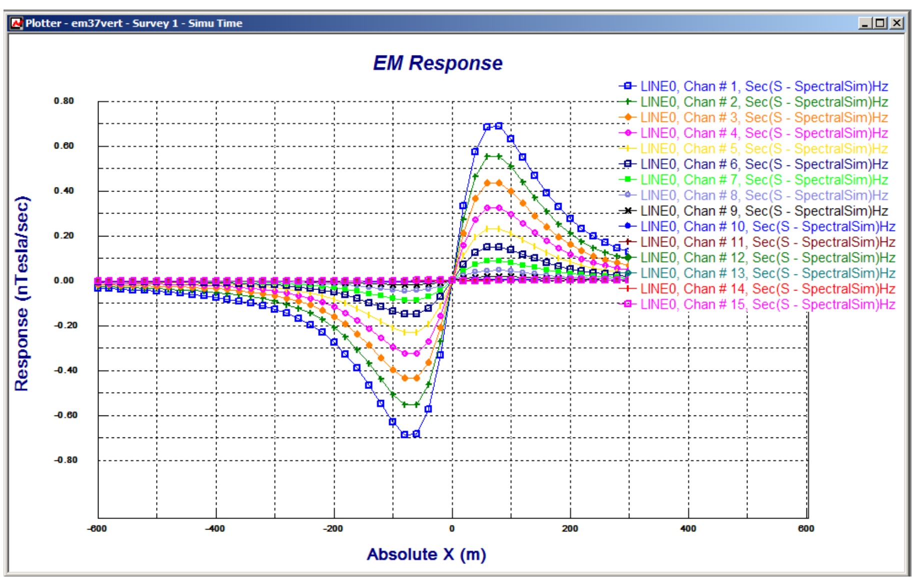

Appendix : Model Parameters

The model parameters were as follows:

Macintosh Directory: RSmithEM37Model

MultiLoop III Files: RSmithEM37-Depth100, RSmithEM37-Depth200, RSmithEM37-Depth50, RSmithEM37-Depth10

Pebble Grid File: PebbleShapeGallery/SingleSurfaces/Plate5x5_131.mcl

Loop Corners: -100,50, 0.1; -200, 50, 0.1, -200,-50,0.1, -100,-50, 0.1

Plate: 100 meters square, 10 S/m; Centered on the profile below 0,0,0, dip 90, strike 90

Background: Nominally resistive

Profile –600,0.1 to 600,0,1 with 61 stations, 20 meters apart

Waveform: Exponential rise, time constant of 0.001 sec; linear turn off 0.001 sec
Offtime 7.3333 msec
Ontime 8.3333 msec
Half period 16.6666 msec (30 Hz base frequency)

Gates:

```
-1      1.000000  1 // NoScalingToTheTimeBase, UnscaledTimeBaseValue,
NormalizeWeightsToDeltaT
//
0            0.000080      0.000096    2     2
// GateName, UnscaledStartTime, UnscaledEndTime, EventIDStart, NumberOfSamples
1       0.000096      0.000117    2     2
2       0.000117      0.000145    2     2
3       0.000145      0.000179    2     2
4       0.000179      0.000223    2     2
5       0.000223      0.000279    2     2
6       0.000279      0.000350    2     2
7       0.000350      0.000441    2     2
8       0.000441      0.000557    2     2
9       0.000557      0.000705    2     2
10      0.000705      0.000894    2     2
11      0.000894      0.001134    2     2
12      0.001134      0.001440    2     2
13      0.001440      0.001831    2     2
14      0.001831      0.002330    2     2
15      0.002330      0.002966    2     2
16      0.002966      0.003779    2     2
17      0.003779      0.004815    2     2
18      0.004815      0.006136    2     2
19      0.006136      0.007333    2     2
```